Supplemental Materials

Interlayer coupling of valley and layer in homostructure bilayer ScI_2

*Xiao-Jing Dong and Chang-Wen Zhang**

School of Physics and Technology, University of Jinan, Jinan, Shandong, 250022, PRC

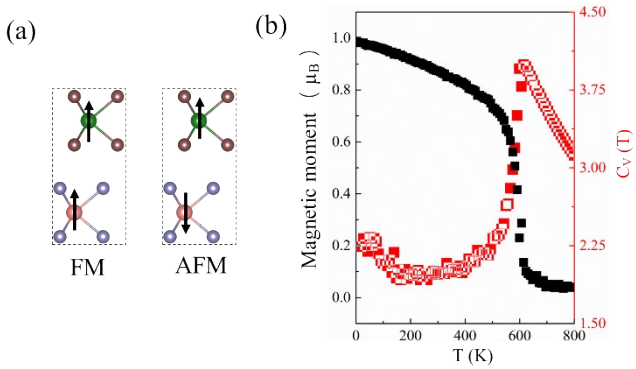

FIG. S1. (a) FM and AFM states of BL ScI_2. (b) Temperature-dependent magnetic moment and specific heat capacity for BL ScI_2.

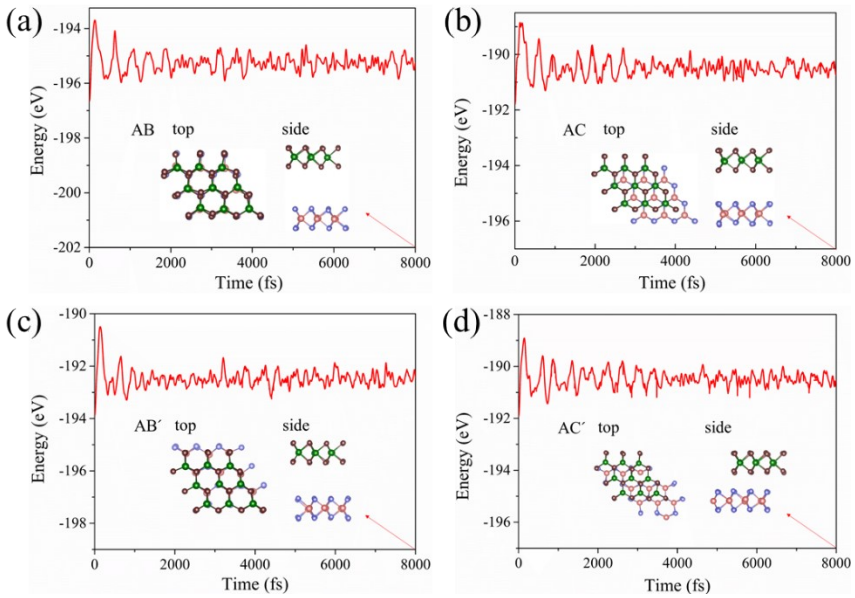

FIG. S2. Free energy evolution during the 8 ps AIMD simulation of BL ScI_2.

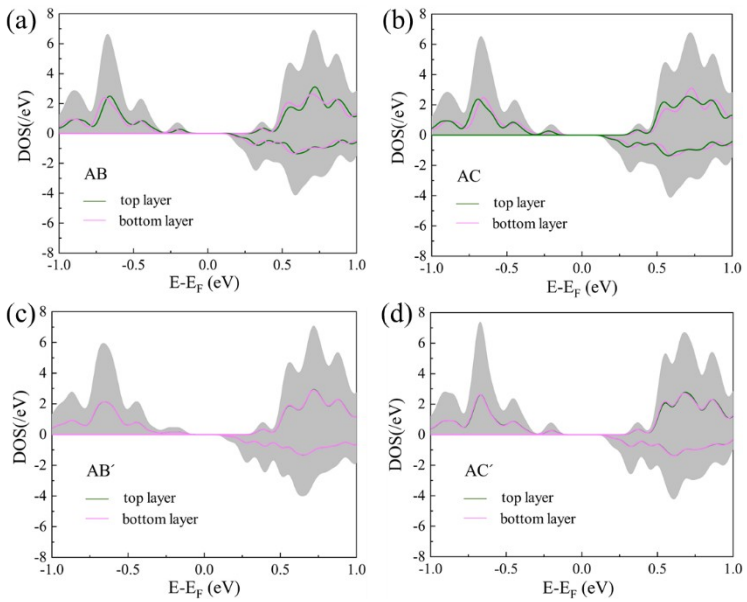

FIG. S3. Density of states for BL ScI_2. The pink/green color corresponds to the bottom/top layer

Tab. S1 Binding energy, interlayer distances and angles in BL ScI_2

Configuration	Binding energy (eV)	Interlayer distances (Å)	I-Sc-I (º) bottom	I-Sc-I (º) top
AB	-1.78	3.46	80.16	80.16
AC	-1.78	3.45	80.22	80.28
AB´	-1.78	3.49	80.26	80.28
AC´	-1.70	4.11	80.30	80.21

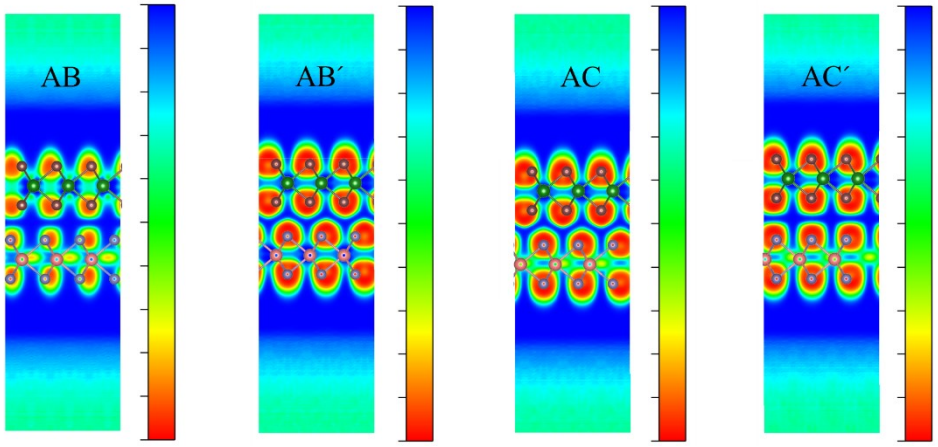

FIG. S4. Electron localization functions of BL ScI_2.

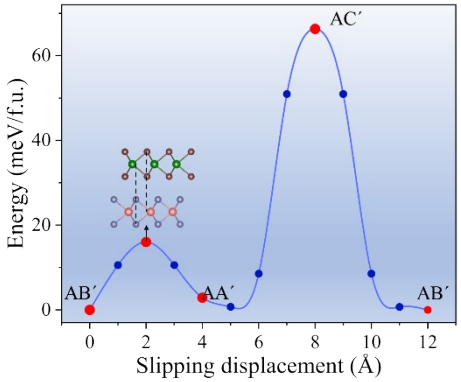

FIG. S5. Energy profiles for FE switching in BL ScI_2.

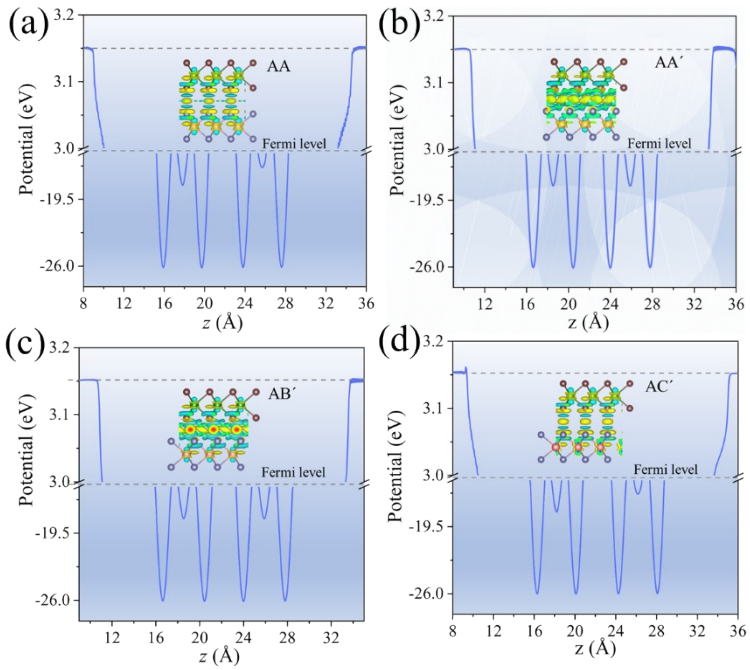

FIG. S6. Plane-averaged electrostatic potentials of (a) AA, (b) AA´, (c) AB´ and (d) AC´ configurations for BL ScI_2 along the *z*-axis. Insets display the corresponding charge densities, with cyan and yellow isosurfaces indicating electron depletion and accumulation, respectively.

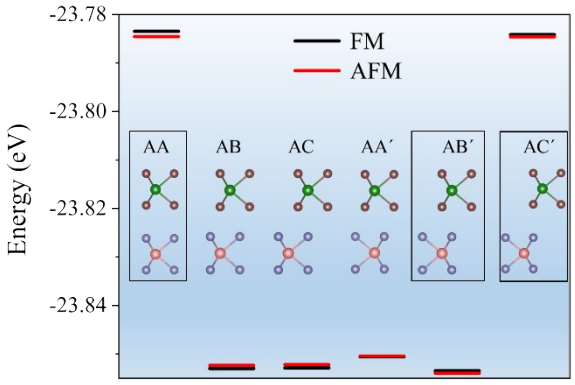

FIG. S7. The energy of six stacking configurations of BL ScI_2 with FM and AFM states.

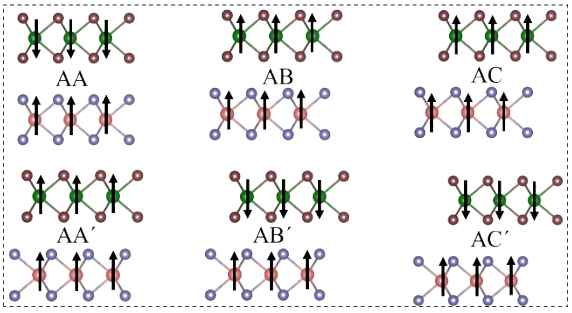

FIG. S8. Six stacking configurations with the magnetic ground states of BL ScI_2.

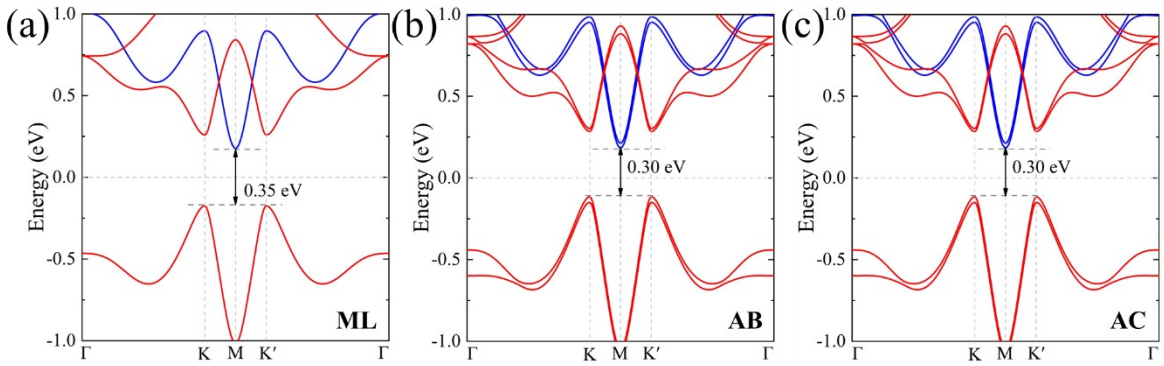

FIG. S9. Spin-polarized band structures without SOC for (a) ML and BL ScI_2 with (b) AB, (c) AC stacking configuration.

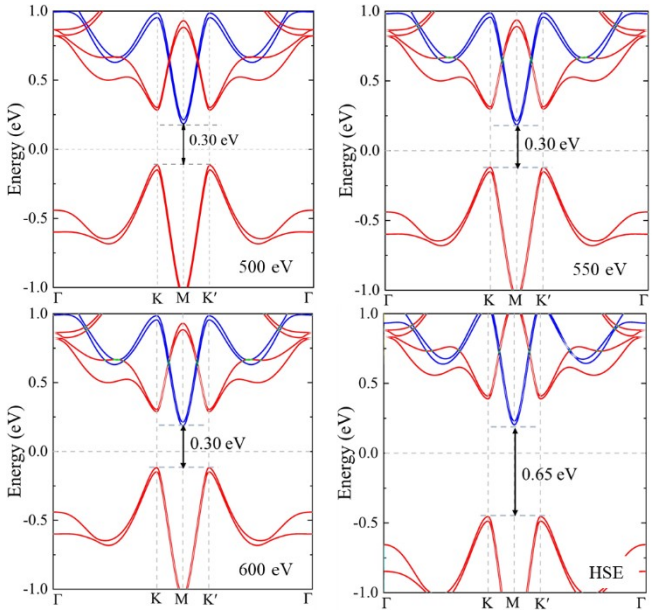

FIG. S10. Spin-polarized band structures without SOC for AB stacking with different cutoff energy (a-c) and HSE function